NCEP RADIATIVE TRANSFER MODEL

Paul van Delst[1], John Derber[2], Tom Kleespies[3], Larry McMillin[3] and Joanna Joiner[4]

[1] National Centers for Environmental Prediction
Cooperative Institute for Meteorological Satellite Studies
Camp Springs MD, USA

[2]National Centers for Environmental Prediction
Environmental Modeling Center
Camp Springs MD, USA

[3]National and Environmental Satellite Data and Information Service
Office of Research and Applications
Climate Research and Applications Division
Camp Springs MD, USA

[4]Goddard Space Flight Center
Data Assimilation Office
Greenbelt MD, USA

1. INTRODUCTION

An essential part of a Numerical Weather Prediction (NWP) data assimilation system incorporating satellite data is the accuracy of the Radiative Transfer Model (RTM) used to simulate instrument observations. Advances in both satellite instrumentation and NWP must be accompanied by similar improvements in the parameterisation of radiative transfer through the atmosphere. This paper details some (ongoing) upgrades to and issues with the RTM currently in use in the NCEP Global Data Assimilation System (GDAS), in preparation for assimilation of AIRS/AMSU/HSB radiances.

2. RADIATIVE TRANSFER MODEL REQUIREMENTS

The goal of the current effort to upgrade the RTM used in the NCEP GDAS is to create a community model for use by NOAA, NASA, and others involved in NWP. This includes supplying all components of an RTM for use in NWP; the forward, tangent-linear, adjoint, and k-matrix models. It also requires that the code be robust enough to work consistently on a variety of platforms running under a variety of operating systems. This implies the use of ANSI/ISO coding standards or, at the very least, to minimise the use of vendor specific language extensions and concentrate them in well documented modules that are loosely coupled to the rest of the code. This reasoning behind this strategy is to make the task of code maintenance and upgrades as simple and painless as possible.

2.1 Operational Issues

One of the operational requirements of the GDAS RTM is that the same code should be used for all satellites/instruments, both infrared (IR) and microwave (MW) sensors. This ensures that the RTM is consistent across all sensors and that any improvements to the RT algorithms automatically apply to all simulated satellite data. Another, not insignificant, benefit of this requirement is that the structure and

application of the code is greatly simplified. That is, different codes are not used for different sensors or combinations of sensors.

Another purely operational requirement is that the RTM should meet NCEP performance and software standards: for a given operational platform the RTM has to be fast enough for data assimilation and should conform to NCEP and Weather Research and Forecast (WRF) coding standards. In addition, NCEP (and likely other NWP centers also) requires upgrades on demand to allow assimilation of new satellite data sources or improve current ones.

2.2 Science Issues

The most important element of any RTM, at least in the context discussed here, is the regression transmittance model. On paper, the choice of which transmittance algorithm to use would be based solely on which model most accurately parameterises the sensor transmittances and physics of atmospheric radiative transfer while simultaneously satisfying the operational requirements. For the operational requirement of "one code for all sensors", the argument can be made that a regression algorithm for one spectral region may not be ideal for another. For example, some experiments suggest that OPTRAN (*McMillin et al,* 1995a,b) has better performance in water vapour regions, but RTATOV (*Saunders and Matricardi*, 1998) performs better in the spectral regions where transmittance is predicted primarily by the fixed gases. However it is not clear whether this performance difference is due to the algorithms themselves or their implementation (the difference most likely being due to interpolation of profile quantities to and from different layering schemes.) This is an issue that needs to be addressed and clarified for the RTM in the GDAS. Currently, NCEP is committed to use of the OPTRAN transmittance algorithm. The ideal assessment solution would allow for the different transmittance algorithms to be simply swapped in and out with no impact on the RTM interface.

The accuracy of a regression RTM model also depends on the accuracy of the monochromatic line-by-line (LBL) transmittances used to in generating the transmittance model regression coefficients. Continua formulations, and spectral line parameters and their formulation change relatively frequently so the LBL transmittances must be regularly updated. For the infrared spectral region, this can involve lengthy computations and prodigious disk space consumption, particular with the advent of high-resolution IR sensors, e.g. AIRS, IASI, and others. The LBL model used to generate the IR transmittances used in the GDAS was LBLRTM (*Clough and Iacono*, 1995) with the HITRAN96 spectral database. A pseudo-LBL IR model, kCARTA (*Strow et al* 1998), may provide a capability for more frequent improvements/changes to spectroscopy formulations coupled with rapid (in an LBL context) recomputation of the monochromatic transmittances.

3. RTM ADDITIONS

3.1 Reflected thermal IR

The operational RTM assumes two things about reflected thermal infrared radiation; firstly that the surface reflectivity is specular and secondly that the upwelling layer transmittance (the transmittance of an individual atmospheric layer) can be used to calculate the downwelling flux layer transmittance. Since, for infrared channels, the surface reflectivity is not typically specular, this is not generally a good approximation. In the upgraded RTM, for infrared channels, the surface reflectivity is always assumed isotropic and the flux transmittance is calculated separately using a diffusivity approximation,

$$\tau_f^{\downarrow} \approx \tau^{\downarrow}(\theta_d) \tag{1}$$

where θ_d, the diffusivity angle, is set to a typical value used for infrared spectral region, $\cos^{-1}$ (3/5) (*De Souza-Machado*, 2000). The combined effect of using the diffuse approximation and assuming isotropic reflectivity is shown in figure 1. It must be noted that the value of the IR surface emissivity used in figure 1, 0.8, is practically non-physical for most IR applications – particularly for the NOAA HIRS instrument. This value is the simply the arbitrary start point of the testing procedure iteration and should be thought of as a worst case number.

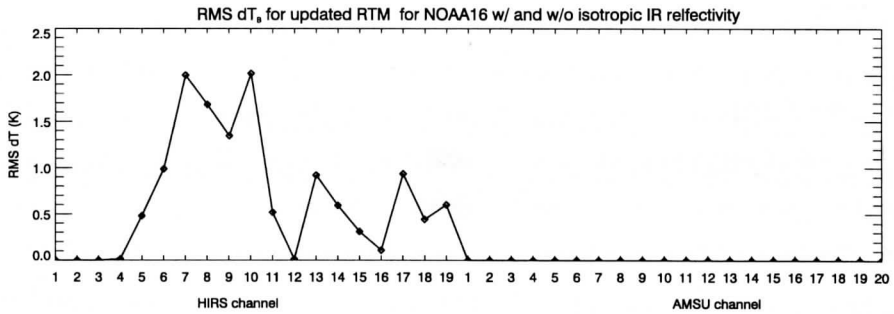

Figure 1 **RMS brightness temperature difference due to isotropic reflectivity of diffuse downwelling thermal flux for the NOAA-16 infrared channels. Surface emissivity is 0.8 (low value explained in text.) 55 profiles were used in the comparison.**

3.2 Microwave cosmic background

The operational RTM does not currently include the cosmic background for the microwave channels. The effect of a cosmic background temperature of T_0=2.736K on the microwave channels assumed specular reflection and a surface emissivity of 0.6 is shown in figure 2. For those microwave channels that view the surface, the effect is non-negligible

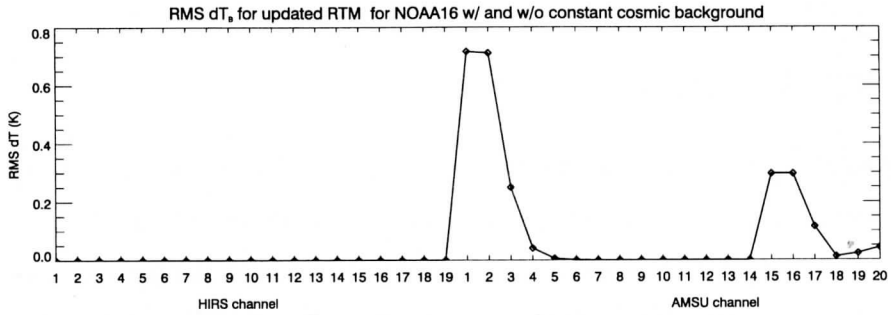

Figure 2 **RMS brightness temperature difference due to a cosmic background temperature of 2.736K assuming specular reflectivity and a surface emissivity of 0.6 for the NOAA-16 infrared and microwave instrument channels. 55 profiles were used in the comparison.**

In some cases the use of a constant cosmic background temperature for the microwave channels is not strictly correct (*Janssen*, 1993). The radiative transfer algorithm in the RTM uses the Planck function to calculate blackbody radiances,

$$B_\nu(T) = \frac{2h\nu^3}{c^2} \cdot \frac{1}{e^{h\nu/kT} - 1} \tag{2}$$

For low frequencies, $h\nu << kT$, the Planck function can be approximated by the Rayleigh-Jeans approximation,

$$B_\nu(T) \approx \frac{2\nu^2 kT}{c^2} \tag{3}$$

The calibration of the NOAA ATOVS AMSU instruments uses the full Planck function (*Mo*, 1995, 1999). When eqn. (3) is used in microwave instrument calibration and eqn. (2) is used to model the microwave instrument then the approximation is no longer valid for cold space temperatures and the higher AMSU frequencies. The effective background temperature then becomes spectrally dependent,

$$T_{0,eff} = \frac{h\nu}{2k} \cdot \frac{e^{h\nu/kT_0} + 1}{e^{h\nu/kT_0} - 1} \tag{4}$$

This is the case with the AMSU/HSB microwave instruments on the EOS Aqua platform (see JPL D-17005, pg32-33.) The impact of this on radiative transfer results (simulated using the NOAA-16 AMSU instrument parameters) is shown in figure 3. The effect is small, and may or may not be negligible when factors such as side-lobe contamination of the cold space calibration view and instrument noise are taken into account.

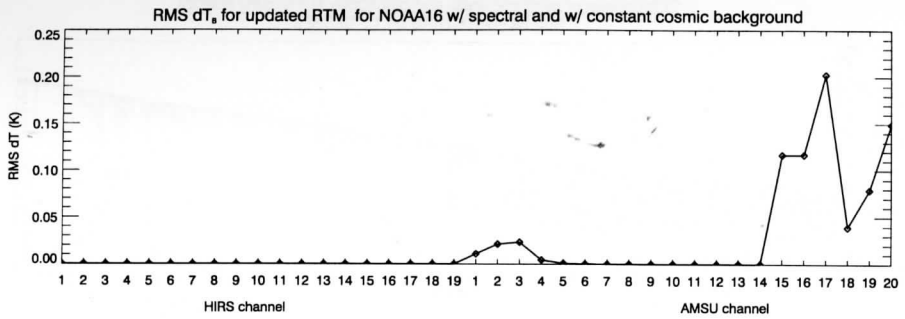

Figure 3 **RMS brightness temperature difference due to a effective cosmic background temperature that is frequency dependent simulated for the NOAA-16 microwave instrument channels. Surface emissivity of 0.6. 55 profiles were used in the comparison.**

3.3 Direct solar contribution

The operational RTM also has no solar component. In incorporating this effect in the upgraded RTM, the synthetic solar spectrum of Kurucz (1992) at the top of the atmosphere (TOA) was compared with that of a blackbody spectrum with a temperature of 5783K. This comparison is shown in the top panel of figure 4 with the affected NOAA-16 HIRS channel spectral response functions (SRFs) superimposed. Apart from the obvious difference in slope of the two source spectra, there are a large number of absorption lines in the 2000-2300cm^{-1} spectral region. This has a greater effect than the slope difference on the convolution of the spectra with the NOAA-16 SRFs – shown in the bottom panel of figure 4. The difference between the convolved values is about 5%.

The convolved synthetic and blackbody values are both accessible in the upgraded RTM. Eventually the user will have the option of specifying which to use but currently the synthetic spectrum values are used with the contribution show in figure 5. As with figure 1, the low IR surface emissivity used (0.8) was for testing purposes only and the results of figure 5 indicate an effectively non-physical worst case. No solar contribution is added if the channel frequency is less than 1800cm^{-1}. This limit will change once high resolution sensor radiances (such as AIRS) are produced, but until then the 1800cm^{-1} limit is sufficient.

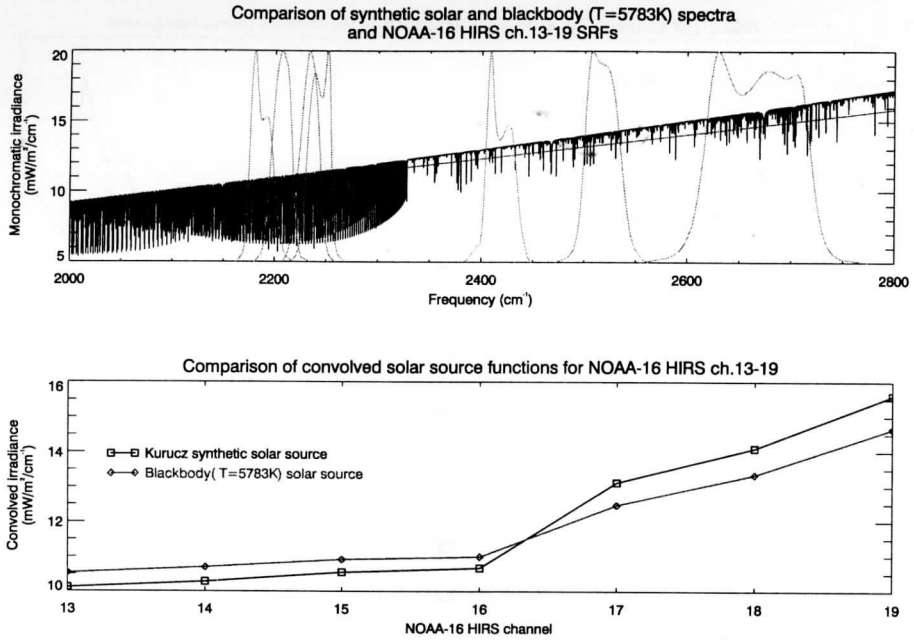

Figure 4 **(*Top*) Comparison of Kurucz synthetic solar and blackbody (T=5783K) spectra at TOA. The NOAA-16 HIRS channel 13-19 SRFs are superimposed. (*Bottom*) Comparison of Kurucz synthetic solar and blackbody (T=5783K) spectra at TOA convolved with the NOAA-16 HIRS channel 13-19 SRFs.**

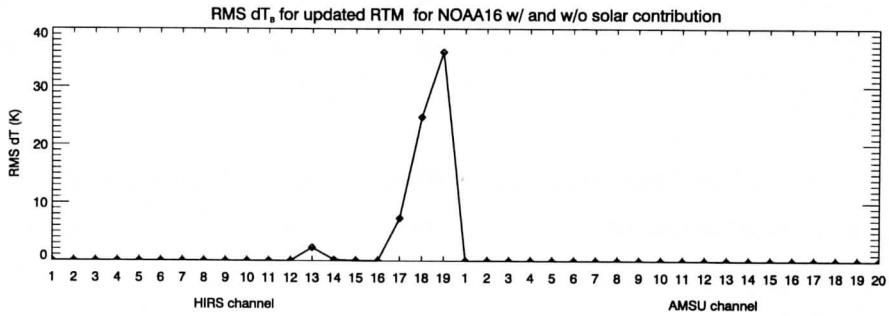

Figure 5 **RMS brightness temperature difference due to direct solar radiation for the NOAA-16 HIRS channels. Surface emissivity of 0.8 (low value explained in text). 55 profiles were used in the comparison.**

4. RTM ISSUES: OPTRAN INTEGRATED PREDICTORS

In defining the OPTRAN predictors currently used in the GDAS RTM, an explicit declaration of the distinction between level and layer quantities should be made. *Level* quantities are interface values, or point measurements, such as radiosonde temperature and water vapour (the sonde sensor response time notwithstanding.) *Layer* quantities are averaged (in some fashion) values between two levels.

In generating coefficients for use in the current GDAS RTM, the integrated predictors used are level valued. The integrated predictors can be written as,

$$X_k^{(m)} = c \cdot \frac{\sum_{i=1}^{k} \left(X_i A_i^m + X_{i-1} A_{i-1}^m \right) \left(A_i - A_{i-1} \right)}{A_k^{m+1}} \tag{5}$$

where $m = 0, 1, 2$, reflecting the order of the integrated predictor,

$k = 1, 2, \ldots, K$, the layer index,

c = order dependent scaling constant,

X_i = level i pressure, p, or level i temperature, T,

A_i = absorber amount integrated to some level i,

$$A_k = \frac{1}{g}\sum_{i=1}^{k} q_i (p_i - p_{i-1}) \tag{6}$$

with q_i = level i absorber concentration, and

p_i = level i pressure with $p_{i-1} = 0.005$hPa.

However, while the GDAS outputs both level and layer pressures, it only supplies average layer temperatures and absorber concentrations for input to the RTM. To accommodate these layer values, the predictor formulations are recast as,

$$\begin{aligned} X_k^{(m)} &\equiv \overline{X}_k^{(m)} + \overline{X}_{k-1}^{(m)} \\ &= c \cdot \frac{\sum_{i=1}^{k} \overline{X}_i \left(\overline{A}_i^m + \overline{A}_{i-1}^m\right)\left(\overline{A}_i - \overline{A}_{i-1}\right)}{\overline{A}_k^{m+1}} + c \cdot \frac{\sum_{i=1}^{k-1} \overline{X}_i \left(\overline{A}_i^m + \overline{A}_{i-1}^m\right)\left(\overline{A}_i - \overline{A}_{i-1}\right)}{\overline{A}_{k-1}^{m+1}} \end{aligned} \tag{7}$$

with,

$$\overline{A}_k = \frac{1}{g}\sum_{i=1}^{k} \overline{q}_i (p_i - p_{i-1}) \tag{8}$$

where the overbar is now used to explicitly represent a *layer* quantity; $\overline{X}_i$ = the average layer i pressure, p, or layer i temperature, T, and $\overline{A}_0$ and $\overline{X}_0^{(m)} = 0$.

The comparison of the temperature integrated predictors specified by equations (5) and (7) are shown in figure 6. The two formulations differ most obviously near the top of the atmosphere above approximately 0.1hPa. It must be noted that the current operational implementation of the OPTRAN transmittance model in the GDAS is based on profiles that extend only to 0.1hPa and the midpoint of the top pressure layer of the GDAS itself is 2hPa (indicated on the plots). The difference between the predictor formulations in that context is negligible in the GDAS RTM – as shown explicitly in figure 7. Below 2hPa the difference between the layer and level predictor value never exceeds 1% and in most cases is much less. It is not yet clear if this will necessarily be the case for future instruments with significantly lower noise levels or if more sophisticated integration techniques for generating the predictor profiles are employed. Of course, changes will become necessary as the model top moves upward.

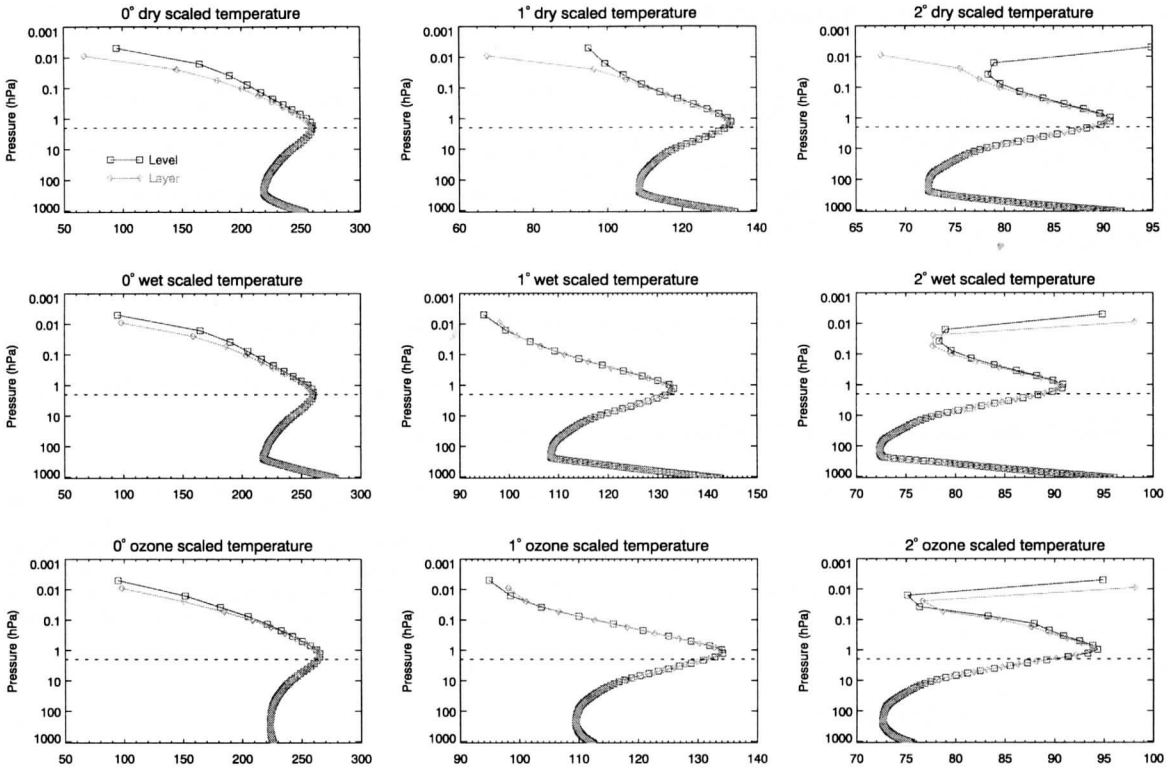

Figure 6. **Comparison of level (eqn.5, ⊠) and layer (eqn.7, ♫) based 0th, 1st, and 2nd order temperature integrated predictors for a test profile with TOA pressure of 0.005hPa. Dotted horizontal line represents midpoint pressure of top layer in the GDAS.**

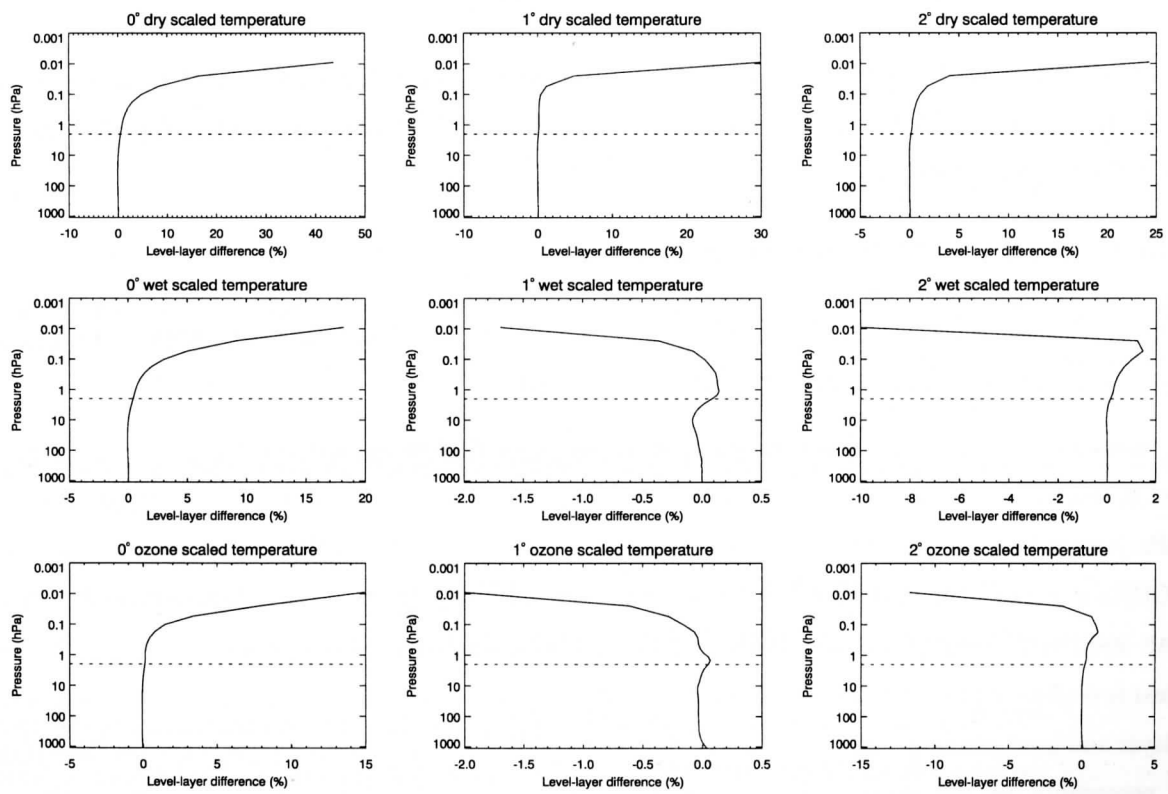

Figure 7. **Percentage difference profiles of level (eqn.5) and layer (eqn.7) based 0th, 1st, and 2nd order temperature integrated predictors for a test profile with TOA pressure of 0.005hPa. Dotted horizontal line represents midpoint pressure of top layer in the GDAS.**

5. CONCLUSIONS AND FURTHER WORK

The current assessment of the operational and upgraded RTM is that the latter (with the same downwelling and surface algorithms, and no solar) has not degraded the results of comparisons between calculated and observed. Further tests to asses the impact of the changes made by adding separate thermal and solar calculations are pending.

The main areas of further work (apart from completing the full suite of RTM components) include:

- Recalculating the transmittance coefficients using layer valued predictors to remove the inconsistency between how the coefficients are generated and how they are used.
- Calculating separate transmittance coefficients for the downwelling (diffuse thermal and solar) transmittance computation. Currently, the layer transmittances determined using coefficients assuming upwelling transmittances and predictors are used to generate the downwelling transmittances.

6. ACKNOWLEDGMENTS

This work was funded under NOAA Grants NA67EC0100 and NA07EC0676.

7. REFERENCES

Clough, S.A. and M.J. Iacono, 1995. Line-by-line calculations of atmospheric fluxes and cooling rates. 2: Applications to carbon dioxide, ozone, methane, nitrous oxide and the halocarbons. *Journal of Geophysical Research*, **100**, pp16519-16535

De Souza-Machado, S., 2000. Private communication.

Hannon, S., L.L. Strow, and W.W. McMillan, 1996. Atmospheric infrared fast transmittance models: A comparison of two approaches. *Proceedings of SPIE*, **2830**, pp94-105.

Janssen, M.A. (ed). Atmospheric Remote Sensing by Microwave Radiometry. John Wiley and Sons, New York, 1993.

JPL D-17005, 10 November 2000, AIRS Project ATBD Level 1b, Part3: Microwave Instruments. Available at: http://eospso.gsfc.nasa.gov/ftp_ATBD/REVIEW/AIRS/atbd-airs-L1B_microwave.pdf

Kurucz, R.L., 1992. Synthetic infrared spectra, pp523-531, Infrared Solar Physics, Proceedings of the 154th Symposium of the International Astronomical Union, M. Rabin, J.T. Jefferies, and C. Lindsey eds. Kluwer Academic Publishers, Dordrecht, 1994.

McMillin, L.M., L.J. Crone, M.D. Goldberg, and T.J. Kleespies, 1995a. Atmospheric transmittance of an absorbing gas. 4. OPTRAN: a computationally fast and accurate transmittance model for absorbing gases with fixed and with variable mixing ratios at variable viewing angles. *Applied Optics*, **34**, pp6269-6274

McMillin, L.M., L.J. Crone, and T.J. Kleespies, 1995b. Atmospheric transmittance of an absorbing gas. 5. Improvements to the OPTRAN approach. *Applied Optics*, **34**, pp8396-8399

Mo, T., Calibration of the Advanced Microwave Sounding Unit-A for NOAA-K, NOAA Technical Report NESDIS 85, U.S. Department of Commerce, Washington, D.C, June 1995

Mo, T, Calibration of the Advanced Microwave Sounding Unit-A Radiometers for NOAA-L and NOAA-M, NOAA Technical Report NESDIS 92, U.S. Department of Commerce, Washington, D.C, May 1999

Saunders, R.W. and M. Matricardi, 1998. A fast forward model for ATOVS (RTATOV). Technical Proceedings 9th International TOVS Study Conference, Igls Austria, 20-26 February.

Strow, L.L., H.E. Motteler, R.G. Benson, S.E. Hannon, and S. De Souza-Machado, 1998. Fast computation of monochromatic infrared atmospheric transmittances using compressed look-up tables. *Journal of Quantitative Spectroscopy and Radiative Transfer*, **59**, pp481-493

TECHNICAL PROCEEDINGS OF THE ELEVENTH INTERNATIONAL ATOVS STUDY CONFERENCE

Budapest Hungary

20-26 September, 2000

Edited by

J.F. Le Marshall and J.D. Jasper

Bureau of Meteorology Research Centre, Melbourne, Australia

Published by

Bureau of Meteorology Research Centre

PO BOX 1289K, GPO Melbourne, Vic., 3001, Australia

June 2001